

AD-A073 077

ROME AIR DEVELOPMENT CENTER GRIFFISS AFB NY
MUTUAL COUPLING EFFECTS ON A CIRCULAR ARRAY OF DIPOLES, (U)
APR 79 G CRUZ

F/G 20/14

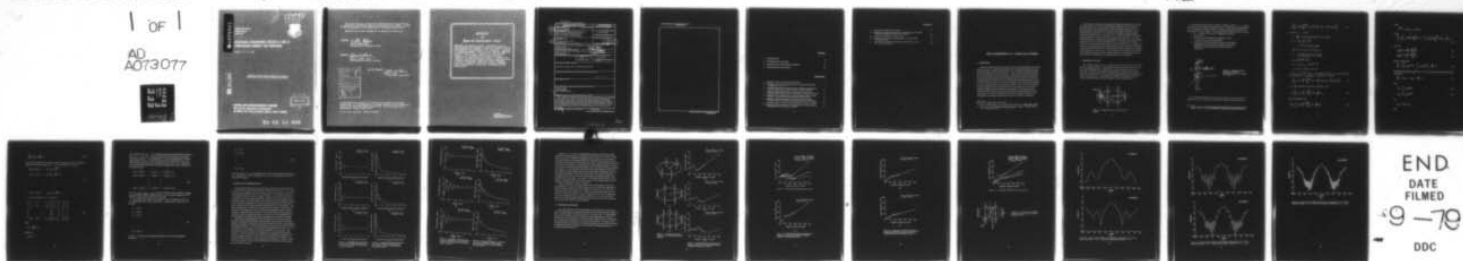
UNCLASSIFIED

RADC-TR-79-82

NL

1 OF 1

AD
A073077





MICROCOPY RESOLUTION TEST CHART
NATIONAL BUREAU OF STANDARDS-1963-A

AD A073077

RADC-TR-79-82

In-House Report

April 1979

MUTUAL COUPLING EFFECTS ON A CIRCULAR ARRAY OF DIPOLES

Gregory Cruz, Lt, USAF

12
P.S.

LEVEL



DDC FILE COPY

APPROVED FOR PUBLIC RELEASE; DISTRIBUTION UNLIMITED

ROME AIR DEVELOPMENT CENTER
Air Force Systems Command
Griffiss Air Force Base, New York 13441

DDC
RECEIVED
AUG 27 1979
A

79 08 24 009

This report has been reviewed by the RADC Information Office (OI) and is releasable to the National Technical Information Service (NTIS). At NTIS it will be releasable to the general public, including foreign nations.

RADC-TR-79-82 has been reviewed and is approved for publication.

APPROVED:

Walter Rotman

WALTER ROTMAN, Chief
Antennas and RF Components Branch

APPROVED:

Allan C. Schell

ALLAN C. SCHELL, Chief
Electromagnetic Sciences Division

Accession for	
NTIS GRA&I	<input checked="" type="checkbox"/>
DDC TAB	<input type="checkbox"/>
Unannounced	<input type="checkbox"/>
Justification	
By _____	
Distribution/	
Availability Codes	
Dist	Availand/or special
<i>A</i>	

FOR THE COMMANDER:

John P. Huss

JOHN P. HUSS
Acting Chief, Plans Office

If your address has changed or if you wish to be removed from the RADC mailing list, or if the addressee is no longer employed by your organization, please notify RADC (EEA) Hanscom AFB MA 01731. This will assist us in maintaining a current mailing list.

Do not return this copy. Retain or destroy.

MISSION of Rome Air Development Center

RADC plans and executes research, development, test and selected acquisition programs in support of Command, Control Communications and Intelligence (C³I) activities. Technical and engineering support within areas of technical competence is provided to ESD Program Offices (POs) and other ESD elements. The principal technical mission areas are communications, electromagnetic guidance and control, surveillance of ground and aerospace objects, intelligence data collection and handling, information system technology, ionospheric propagation, solid state sciences, microwave physics and electronic reliability, maintainability and compatibility.

Printed by
United States Air Force
Hanscom AFB, Mass. 01731

Unclassified

SECURITY CLASSIFICATION OF THIS PAGE (When Data Entered)

REPORT DOCUMENTATION PAGE		READ INSTRUCTIONS BEFORE COMPLETING FORM
1. REPORT NUMBER RADC-TR-79-82	2. GOVT ACCESSION NO.	3. REPORT'S CATALOG NUMBER
4. TITLE (and Subtitle) MUTUAL COUPLING EFFECTS ON A CIRCULAR ARRAY OF DIPOLES		5. TYPE OF REPORT & PERIOD COVERED In-House Report
7. AUTHOR(s) Gregory/Cruz, Lt, USAF		6. PERFORMING ORG. REPORT NUMBER
9. PERFORMING ORGANIZATION NAME AND ADDRESS Deputy for Electronic Technology (RADC/EEA) Hanscom AFB Massachusetts 01731		8. CONTRACT OR GRANT NUMBER(s)
11. CONTROLLING OFFICE NAME AND ADDRESS Deputy for Electronic Technology (RADC/EEA) Hanscom AFB Massachusetts 01731		10. PROGRAM ELEMENT, PROJECT, TASK AREA & WORK UNIT NUMBERS 23050393
14. MONITORING AGENCY NAME & ADDRESS (if different from Controlling Office) 12 23 p.		13. REPORT DATE April 1979
		15. SECURITY CLASS. (of this report) Unclassified
		15a. DECLASSIFICATION/DOWNGRADING SCHEDULE
16. DISTRIBUTION STATEMENT (of this Report) Approved for public release; distribution unlimited.		
17. DISTRIBUTION STATEMENT (of the abstract entered in Block 20, if different from Report) 611 027		
18. SUPPLEMENTARY NOTES		
19. KEY WORDS (Continue on reverse side if necessary and identify by block number) Circular array Mutual coupling Active element pattern		
20. ABSTRACT (Continue on reverse side if necessary and identify by block number) An analysis of coupled dipoles based on integral equations for currents that must be satisfied in order to meet the boundary conditions along the surface of the elements. The computer is used to numerically solve the M nonhomogeneous integral equations, using numerical approximations for the integrals and complex algebra techniques to solve the simultaneous equations. Such an analysis displays the mutual and self-admittance characteristics of a circular array and determines the effects of mutual coupling on the active element pattern.		

DD FORM 1 JAN 73 1473

EDITION OF 1 NOV 65 IS OBSOLETE

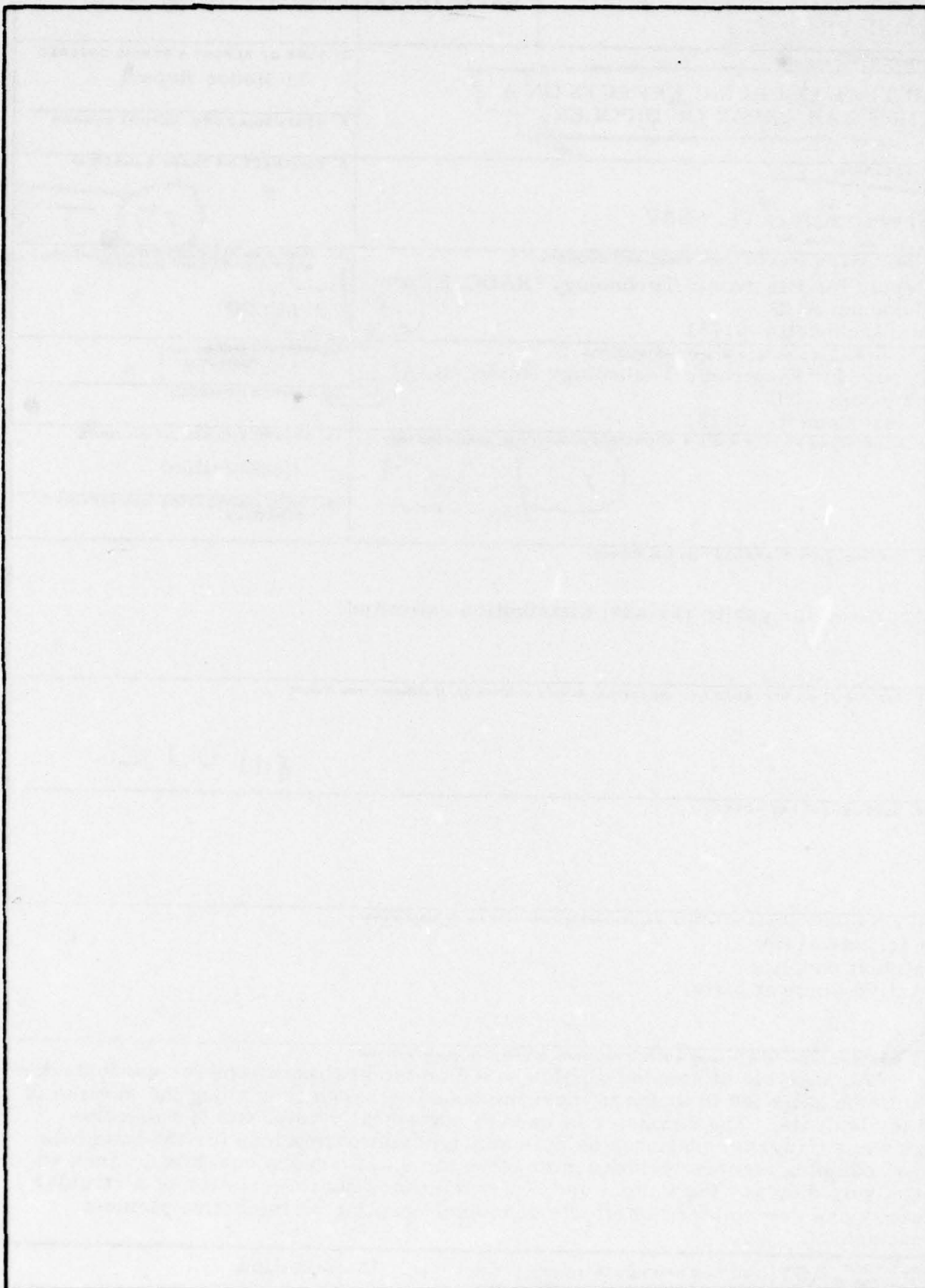
Unclassified

SECURITY CLASSIFICATION OF THIS PAGE (When Data Entered)

309050

Em

Unclassified
SECURITY CLASSIFICATION OF THIS PAGE(When Data Entered)



Unclassified
SECURITY CLASSIFICATION OF THIS PAGE(When Data Entered)

Contents

1. INTRODUCTION	5
2. MATHEMATICAL ANALYSIS	6
3. PRESENTATION OF NUMERICAL RESULTS	12
4. DISCUSSION AND CONCLUSION	15

Illustrations

1. Perspective View of Circular Array Antenna	6
2. Cylindrical Dipole, Showing the Method of Applying the Boundary Condition $E_z = 0$ at $r = a$	7
3. Magnitude of Self Admittance for Varying of Interelemental Spacing While Holding Number of Elements and Frequency Constant	13
4. Magnitude of Mutual Admittance for Varying of Interelemental Spacing While Holding Number of Elements and Frequency Constant	13
5. Magnitude of Self Admittance for Varying Frequency While Holding Number of Elements and Interelemental Spacing Constant	14
6. Magnitude of Mutual Admittance for Varying Frequency While Holding Number of Elements and Interelemental Spacing Constant	14
7. Varying the Number of Elements While Holding the Radius Constant	16
8. Magnitude of Self Admittance for Varying Number of Elements While Holding Radius and Frequency Constant	16

Illustrations

9. Composite of Figures 8a, 8b, and 8c	17
10. Magnitude of Mutual Admittance for Varying Number of Elements While Holding Radius and Frequency Constant	17
11. Composite of Figures 10a, 10b, and 10c	19
12. Circular Array Showing Coordinate System Used in Finding Radiation Pattern	19
13. Active Element Patterns for Circular Arrays With 6, 10, 30, 50, and 100 Elements	20

Mutual Coupling Effects on a Circular Array of Dipoles

1. INTRODUCTION

Studies of coupled antennas for circular arrays may be separated into two groups: those that assume a convenient distribution of current along each identical element regardless of their relative locations in the array, and those that attempt to obtain the actual currents in the several elements. Nearly all of the early and most of the more recent analyses are in the first group, in which both field patterns and impedances have been determined for elements with assumed currents. An analysis of coupled antennas from the point of view of finding the actual distributions of currents for the N-element circular array was done by King¹ in 1950, and a general analysis of arrays of coupled antennas was also done by King.² This is done by formulation of integral equations for the currents that must be satisfied in order to meet the boundary conditions along the surfaces of the elements. The drawback of this method is that the rigorous solution of the simultaneous integral equations for the distributions of current in the elements of the array of parallel elements is very complicated and no simple and practically useful set of formulas is obtained.

(Received for publication 17 April 1979)

1. King, R. (1950) Theory of N-coupled parallel antennas, J. Appl. Phys. 21:94.
2. King, R.W.P. (1958) Theory of Linear Antennas, Chapter 3, Harvard University, Cambridge, MA.

In this report we shall use the techniques of King for the derivation of the integral equations for the currents, and from this starting point use the computer to numerically solve the M nonhomogeneous integral equations (using numerical approximations for the integrals and complex matrix algebra techniques to solve the simultaneous equations). Such an analysis will display the mutual and self admittance characteristics of a circular array. We shall investigate the effects of mutual coupling for a circular array with a single active element by: (1) varying the distance of the circumferential spacing between adjacent elements while keeping the frequency and the number of elements in the array constant; (2) varying the frequency while keeping the radius and the number of elements in the circular array constant; (3) varying the number of elements in the circular array while keeping the radius and frequency constant; and (4) generating the radiation pattern for a single active element of a circular array. Such a study will have an impact on the development of optimum methods for determining techniques for radiation pattern generation with very low sidelobes and a minimum number of array elements.

2. MATHEMATICAL ANALYSIS

The circular antenna array to be considered (see Figure 1) consists of identical, parallel, cylindrical dipoles equally spaced around the circumference of a circle. Only center-fed dipoles with a half length $h = \lambda/4$ and a radius a will be used as elements. The center of each dipole is perpendicular to the plane of the circle. Each of the elements of the array is thus in the same geometrical environment. The radius of the circle is ρ . The electrical circumference of the circle is then $\beta\rho$, where β is defined in terms of the wavelength λ by the relationship $2\pi/\lambda$.

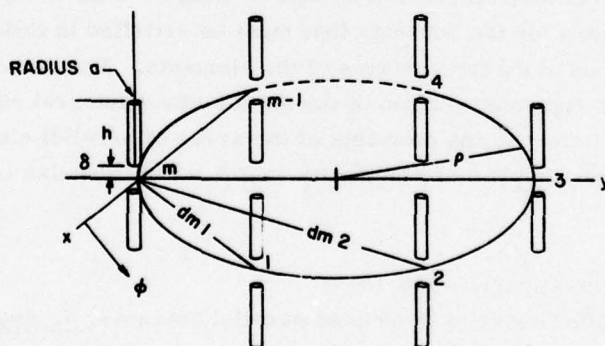


Figure 1. Perspective View of Circular Array Antenna

Let each dipole of the array be driven by a voltage V_i where $i = 1, \dots, m$ and m is the number of elements in the circular array. A physically realizable element has a base gap where voltage is applied. We will assume a base gap width of 2δ (see Figure 2) for this analysis. From the geometrical pattern of Figure 1 assume:

1. $\beta a \ll 1$ (there will be only a Z-component of current in each antenna).
2. The end faces of the antenna are neglected, and the current is taken as zero at both ends.
3. If assumed elements are perfect conductors, the boundary condition that must be satisfied is that the electric field tangential to each element on its cylindrical surface must be zero.

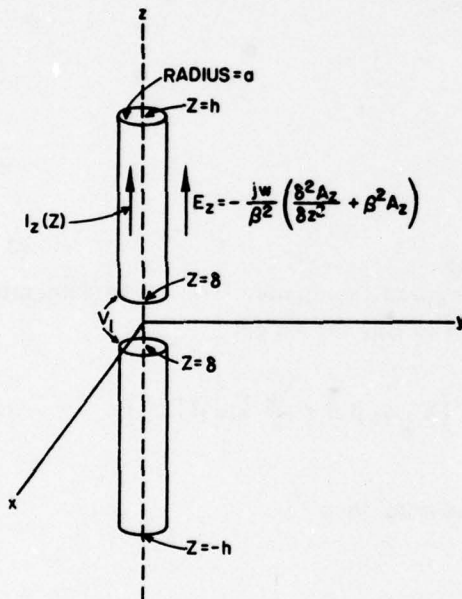


Figure 2. Cylindrical Dipole, Showing the Method of Applying the Boundary Condition $E_z = 0$ at $r = a$

It is readily shown³ that the currents on the circular array of m elements are related to the m base voltages by m simultaneous integral equations similar to

3. Tillman, James D. (1966) The Theory and Design of Circular Antenna Arrays, Chapter 1, The University of Tennessee, Engineering Experiment Station.

$$\int_{-h}^h \sum_{i=1}^m I_{zi}(Z) \frac{e^{-j\beta R_{ki}}}{R_{ki}} dZ = \frac{-j4\pi}{\eta} \left(k \cos \beta Z + \frac{V_k}{2} \sin \beta |Z| \right) \quad (1)$$

for each $K = 1, \dots, m$ where

$\eta = \sqrt{\frac{\mu}{\epsilon}}$ is the intrinsic impedance of free space,

$$\beta^2 = \frac{W^2}{\mu\epsilon} = \frac{W^2}{C^2} = \left(\frac{2\pi}{\lambda}\right)^2$$

$C = 1/\sqrt{\mu\epsilon}$ is the speed of light,

$I_{zi}(Z)$ is the current on the i^{th} element,

d_{mi} is the distance from the i^{th} element to the m^{th} element in the Z plane,

$$R_{mi} = \sqrt{(Z - Z_i)^2 + d_{mi}^2}$$

$$\text{and if } i = m \text{ then } R_{mm} = \sqrt{(Z - Z)^2 + a^2}$$

V_k is the base voltage for element K .

Let $I_{zi} = A_i \cos \frac{KZ}{L}$, where L is the length of the dipole. We are to determine these coefficients A_i . Substituting for $I_{zi}(Z)$ in Eq. (1) we get

$$\int_{-h}^h \sum_{i=1}^m A_i \cos \frac{\pi Z}{L} \frac{e^{-j\beta R_{ki}}}{R_{ki}} dZ = \frac{-j4\pi}{\eta} \left(k \cos \beta Z + \frac{V_k}{2} \sin \beta |Z| \right) \quad (2)$$

Let $Z = \frac{K}{2\beta}$ to simplify the right-hand expression, then

$$\int_{-h}^h \sum_{i=1}^m A_i \cos \frac{\pi Z}{L} \frac{e^{-j\beta R_{ki}}}{R_{ki}} dZ = \frac{-j4\pi}{2\eta} V_k \quad (3)$$

Upon rearranging we get

$$\sum_{i=1}^m A_i \int_{-h}^h \cos \frac{\pi Z}{L} \frac{e^{-j\beta R_{ki}}}{R_{ki}} dZ = \frac{-j4\pi}{2\eta} V_k \quad (4)$$

Using

$$e^{-j\beta R_{ki}} = \cos \beta R_{ki} - j \sin \beta R_{ki},$$

we get

$$\sum_{i=1}^m A_i \left\{ \int_{-h}^h \cos \frac{\pi Z}{L} \frac{\cos \beta R_{ki}}{R_{ki}} dZ - j \int_{-h}^h \cos \frac{\pi Z}{L} \frac{\sin \beta R_{ki}}{R_{ki}} dZ \right\} = \frac{-j2\pi}{\eta} V_k. \quad (5)$$

Now, let

$$f_{1ki}(Z) = \cos \frac{\pi Z}{L} \frac{\cos \beta R_{ki}}{R_{ki}} \quad (6)$$

$$f_{2ki}(Z) = \cos \frac{\pi Z}{L} \frac{\sin \beta R_{ki}}{R_{ki}}, \quad (7)$$

then Eq. (5) becomes

$$\sum_{i=1}^m A_i \left\{ \int_{-h}^h f_{1ki}(Z) dZ - j \int_{-h}^h f_{2ki}(Z) dZ \right\} = \frac{-j2\pi}{\eta} V_k. \quad (8)$$

We integrate $f_{1ki}(Z)$ and $f_{2ki}(Z)$ from $-h$ to h by using cautious Romberg extrapolation to yield

$$\sum_{i=1}^m A_i \left\{ F_{1ki} - j F_{2ki} \right\} = \frac{-j2\pi}{\eta} V_k \quad (9)$$

where

$$F_{1ki} = \int_{-h}^h f_{1ki}(Z) dZ \quad (10)$$

$$F_{2ki} = \int_{-h}^h f_{2ki}(Z) dZ. \quad (11)$$

Let

$$F_{1ki} - j F_{2ki} = T_{ki}$$

then

$$\sum_{i=1}^m A_i T_{ki} = \frac{-j2\pi}{\eta} V_k. \quad (12)$$

Now we shall consider the M integral equations by taking a look at the equations yielded for each base voltage V_k ($K = 1, \dots, m$) simultaneously. We get

$$\begin{aligned} A_1 T_{11} + A_2 T_{12} + \dots + A_m T_{1m} &= \frac{-j2\pi}{\eta} V_1 \\ A_1 T_{21} + A_2 T_{22} + \dots + A_m T_{2m} &= \frac{-j2\pi}{\eta} V_2 \\ \cdot & \quad \cdot \quad \dots \quad \cdot = \cdot \\ \cdot & \quad \cdot \quad \dots \quad \cdot = \cdot \\ \cdot & \quad \cdot \quad \dots \quad \cdot = \cdot \\ A_1 T_{m1} + A_2 T_{m2} + \dots + A_m T_{mm} &= \frac{-j2\pi}{\eta} V_m. \end{aligned} \quad (13)$$

In a matrix notation Eq. (13) is equal to

$$\begin{bmatrix} T_{11} & T_{12} & \dots & T_{1m} \\ T_{12} & T_{22} & \dots & T_{2m} \\ \cdot & & \dots & \\ \cdot & & \dots & \\ \cdot & & \dots & \\ T_{m1} & T_{m2} & \dots & T_{mm} \end{bmatrix} \begin{bmatrix} A_1 \\ A_2 \\ \cdot \\ \cdot \\ \cdot \\ A_m \end{bmatrix} = \begin{bmatrix} \tilde{V}_1 \\ \tilde{V}_2 \\ \cdot \\ \cdot \\ \cdot \\ \tilde{V}_m \end{bmatrix} \quad (14)$$

where

$$\tilde{V}_k = \frac{-j2\pi}{\eta} V_K.$$

Therefore,

$$\vec{T} \vec{A} = \vec{\tilde{V}}.$$

Given values for $\tilde{V}_1, \tilde{V}_2, \dots, \tilde{V}_m$ and having numerically approximated the integrals T_{ki} ($i = 1, \dots, m; K = 1, \dots, m$), we compute the values for the A_i 's by factoring the matrix T into the $L - U$ decomposition of a row-wise permutation of T and solving the systems of Eq. (5). Once the values for the A_i 's have been found, we can then determine the mutual and self admittances of the circular array. Equation (1) gives the relationship between the currents and voltages of the array elements. For a m -element array,

$$\begin{aligned}
 Y_{11}V_1 + Y_{12}V_2 + \dots + Y_{1k}V_k + \dots + Y_{1m}V_m &= I_1 \\
 Y_{21}V_1 + Y_{22}V_2 + \dots + Y_{2k}V_k + \dots + Y_{2m}V_m &= I_2 \\
 \cdot &\dots \cdot \dots \cdot \\
 \cdot &\dots \cdot \dots \cdot \\
 \cdot &\dots \cdot \dots \cdot \\
 Y_{m1}V_1 + Y_{m2}V_2 + \dots + Y_{mk}V_k + \dots + Y_{mm}V_m &= I_m
 \end{aligned} \tag{16}$$

where $Y_{11}, Y_{22}, \dots, Y_{kk}, \dots, Y_{mm}$ are the self admittance of the respective element, Y_{ab} is the mutual admittance between a and b , V_K is the applied voltage on the K^{th} element, and I_K is the current in the K^{th} element.

For an array with a single active element, which for simplicity's sake we let be element number one, every V_K where $K \neq 1$ is equal to zero. Thus, Eq. (16) becomes

$$\begin{aligned}
 I_1 &= Y_{11}V_1 \\
 I_2 &= Y_{21}V_1 \\
 I_3 &= Y_{31}V_1 \\
 \cdot & \\
 \cdot & \\
 \cdot & \\
 \cdot & \\
 I_m &= Y_{m1}V_1
 \end{aligned} \tag{17}$$

We let $V_1 = 1$ and A_K is the magnitude and phase of the current on element K . Therefore,

$$A_1 = Y_{11}$$

$$A_2 = Y_{21}$$

.

.

.

.

$$A_m = Y_{m1}$$

(18)

Thus, the coefficient A_1 is the self admittance of the active element number one and the coefficient A_K , where K is unequal to one, is the mutual admittance between the first and K^{th} element.

3. PRESENTATION OF NUMERICAL RESULTS

Mutual and self admittances were determined through use of computer programs to numerically solve the M nonhomogeneous simultaneous equations [Eq. (13)]. Figure 3 shows the magnitude of the self admittance of the active element as the distance between adjacent elements varies up to 5 wavelengths. In each case the frequency (1.3 GHz) and array size were held constant. Figures 3a, 3b, and 3c show that the magnitude of the self admittance approaches a common value with increase in inter-elemental spacing. This characteristic value was found not to be frequency dependent. Figure 4 shows the magnitude of the mutual admittance between the active element and an adjacent element as interelemental spacing varies up to 5 wavelengths. Once again the frequency (1.3 GHz) and array size were held constant. Under these conditions the mutual admittance rapidly decreased as the distance between elements increased. Regardless of the array size, the mutual admittance value approached a common value as separation increased. As in the case for the magnitude of the self admittance, the characteristic value was found not to be frequency dependent.

The self and mutual admittances were calculated for a particular array size, holding the spacing between adjacent elements constant while varying the frequency. Figures 5 and 6 show the magnitude of the self and mutual admittance characteristics under these conditions. For the self admittance case for the active element (Figure 5), it is seen that as the frequency is increased the self admittance values for a 2-, 10-, and 50-element array (Figures 5a, 5b, and 5c) approach a common value. This characteristic value was found to be independent of the spacing between adjacent elements. Figure 6 shows that as the frequency is increased the magnitude of the mutual admittance decreases. This is due to the fact that as the frequency is increased the distance between adjacent elements in wavelengths is increased. Again the curves approach a common value independent of the array size and the spacing between adjacent elements.

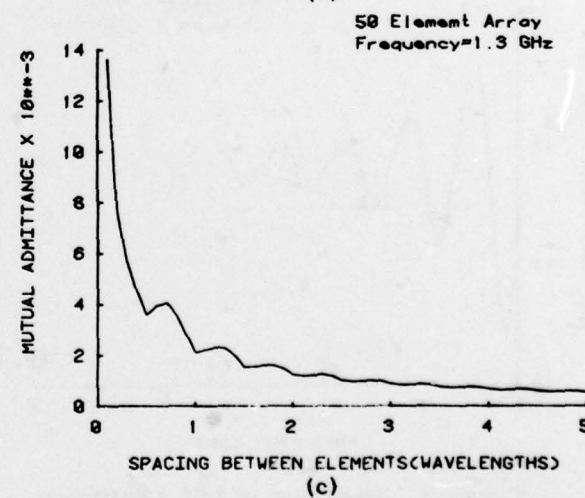
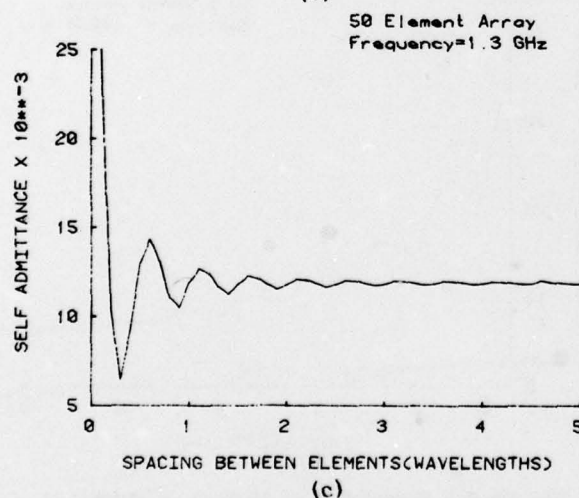
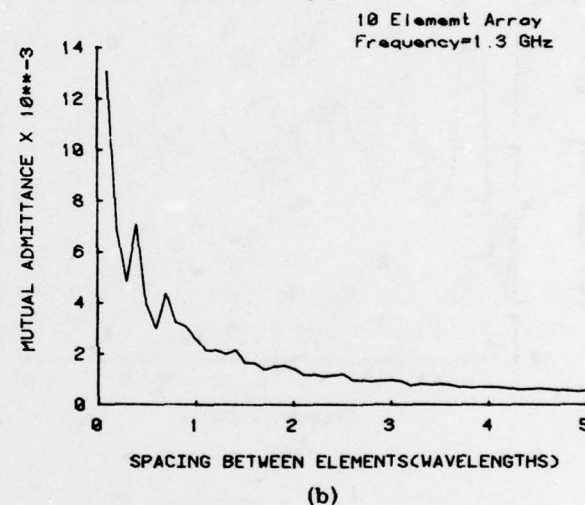
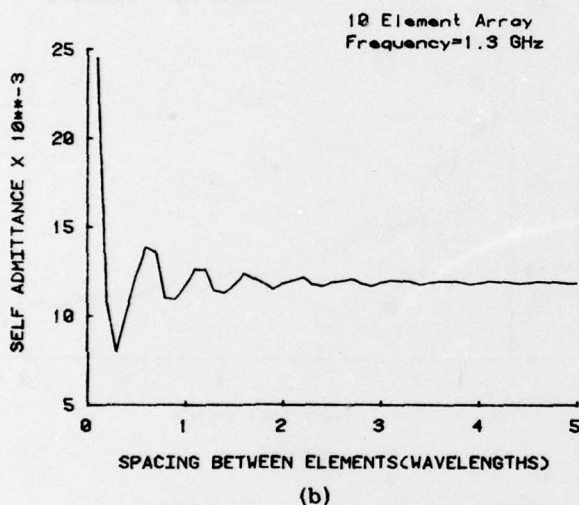
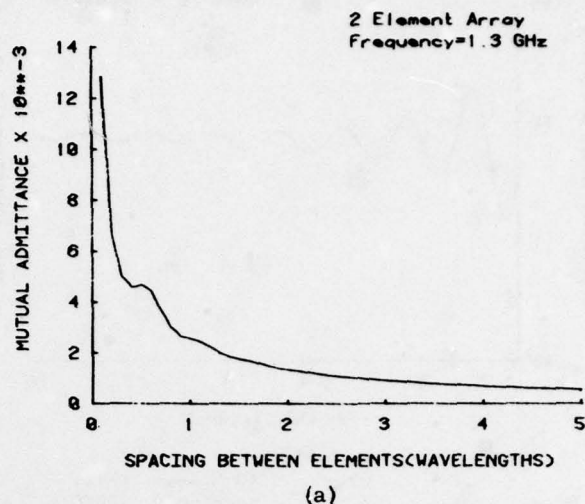
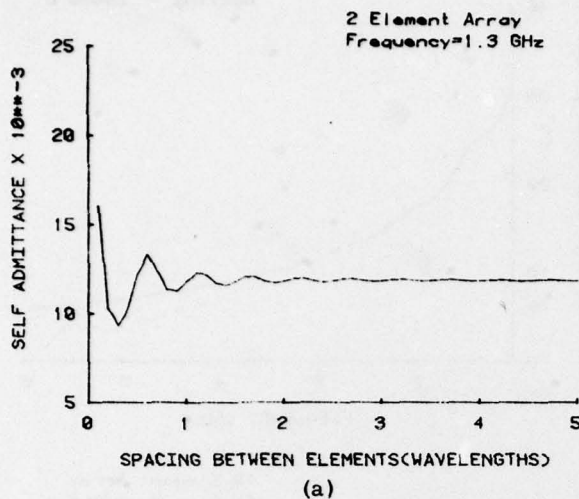
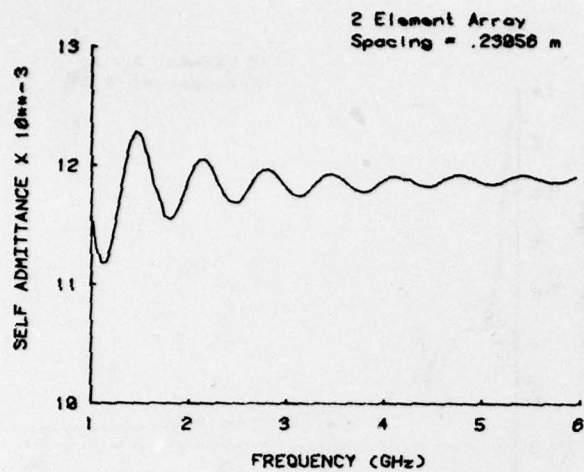
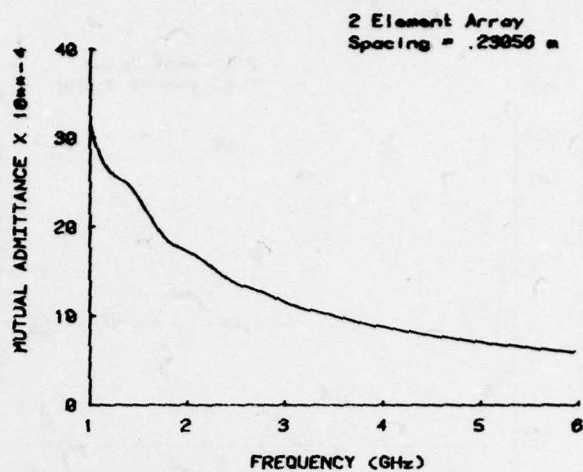


Figure 3. Magnitude of Self Admittance for Varying of Interelemental Spacing While Holding Number of Elements and Frequency Constant

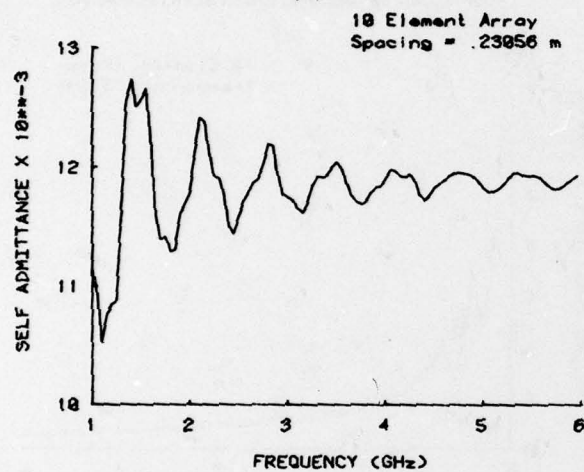
Figure 4. Magnitude of Mutual Admittance for Varying of Interelemental Spacing While Holding Number of Elements and Frequency Constant



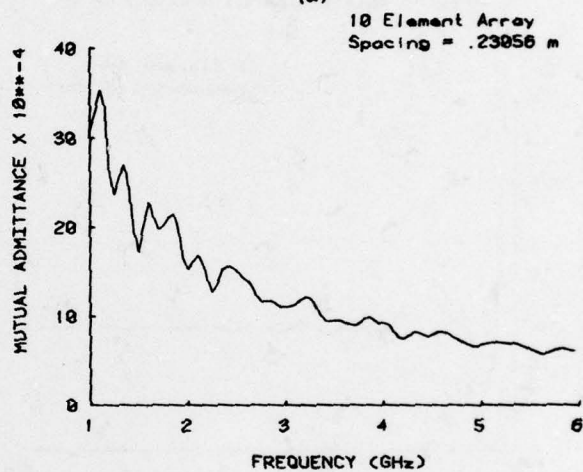
(a)



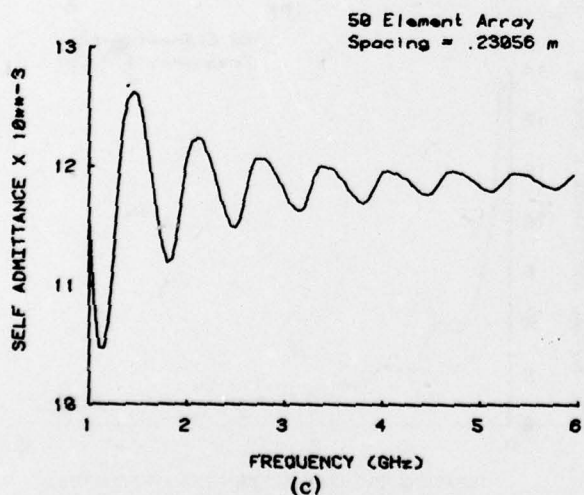
(a)



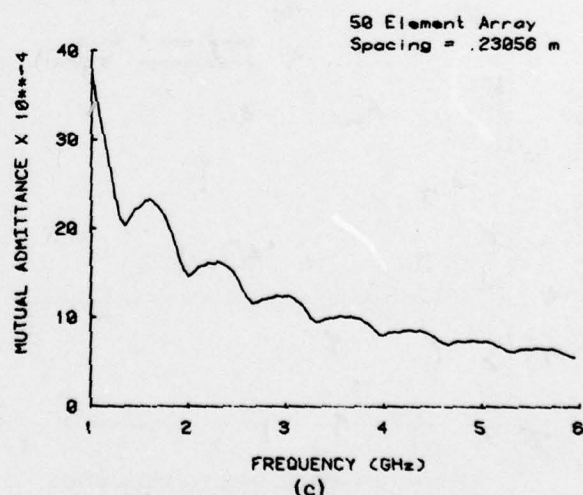
(b)



(b)



(c)



(c)

Figure 5. Magnitude of Self Admittance for Varying Frequency While Holding Number of Elements and Interelemental Spacing Constant

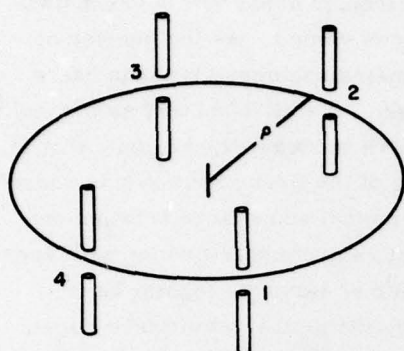
Figure 6. Magnitude of Mutual Admittance for Varying Frequency While Holding Number of Elements and Interelemental Spacing Constant

Figures 7, 8, 9, 10, and 11 illustrate the magnitude of the self and mutual admittances when the frequency and radius of the circular array are held constant while the number of elements comprising the array is varied. As the number of elements is increased, the spacing between the elements becomes less than half a wavelength and the curve becomes linear at the right. It was found that as the radius of the array was increased, the self admittance curve tended to spread out, that is, the second peak value was diminished and the slope of the linear section was reduced (see Figure 9). Similar results were found in the mutual admittance between the active element and an adjacent element for constant radius and frequency with varying number of elements. With the increased number of elements forcing interelemental spacing to be less than half a wavelength, the mutual admittance curve becomes linear to the right, as in Figure 10. For different radius values, as the radius is increased the slope of the linear portion of the mutual admittance curve is reduced (less positive), as seen in Figure 11.

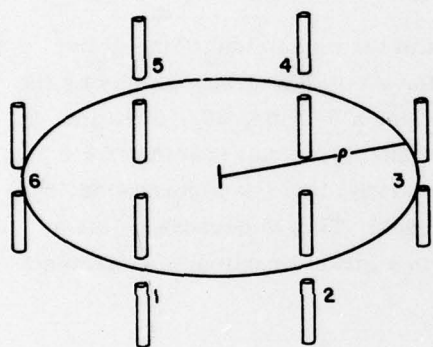
Figure 12 shows the coordinate system used in the calculation of the active element patterns. The active element patterns for a circular array displaying the effects of mutual coupling are shown in Figure 13 for a 6-, 10-, 30-, 50-, and 100-element array at a frequency of 1.3 GHz and interelemental spacing of 0.5λ . With an increase in the number of elements in the array, there is a corresponding increase in the backlobe and the number of sidelobes. This is because unlike a planar array whose elements contribute equally in a given direction, the elements of a circular array point in various directions.

4. DISCUSSION AND CONCLUSION

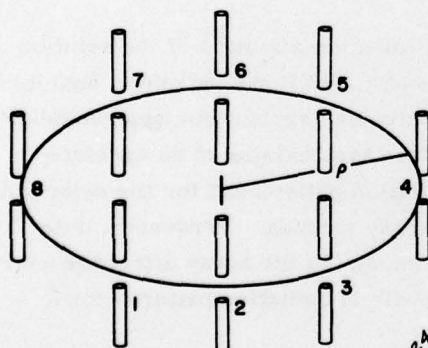
It has been shown that numerical techniques for approximation of the solution of the M nonhomogeneous simultaneous equations [Eq. (13)] provide useful analytical data in the determination of characteristics of a circular array. An understanding of the effects of mutual coupling is necessary in the synthesizing of an aperture distribution to give the best fit to a specified radiation pattern and for the determination of optimization techniques for the circular array antenna. Frequency, interelemental spacing, and the number of elements comprising the array affect the degree of coupling and should be considered in the synthesis of radiation patterns for a specified illumination function.



(a)



(b)



(c)

Figure 7. Varying the Number of Elements While Holding the Radius Constant

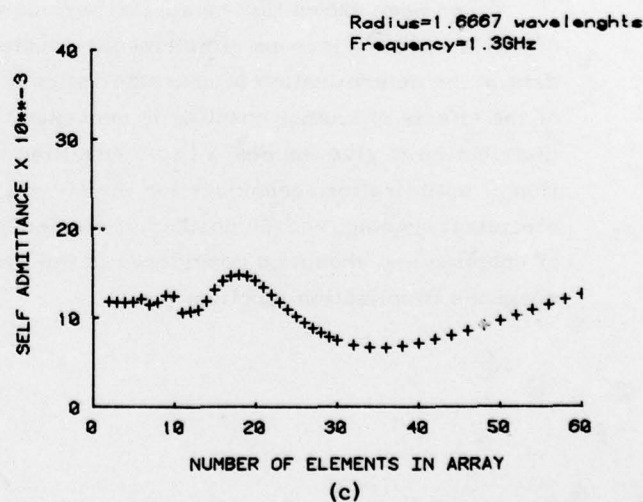
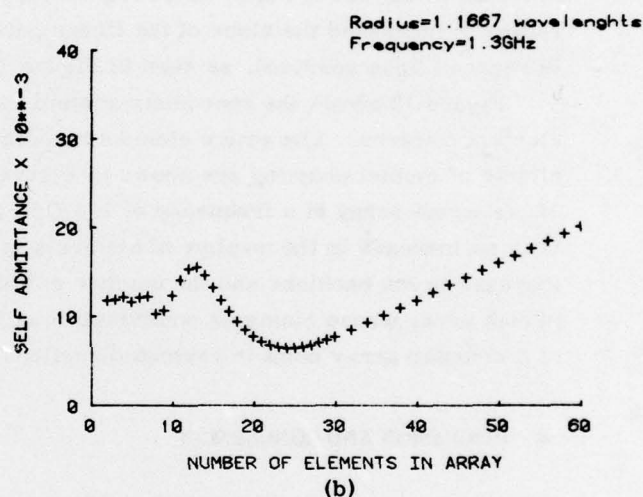
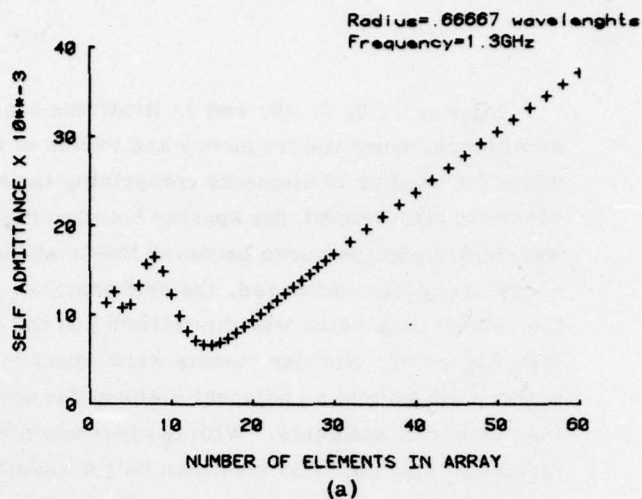


Figure 8. Magnitude of Self Admittance for Varying Number of Elements While Holding Radius and Frequency Constant

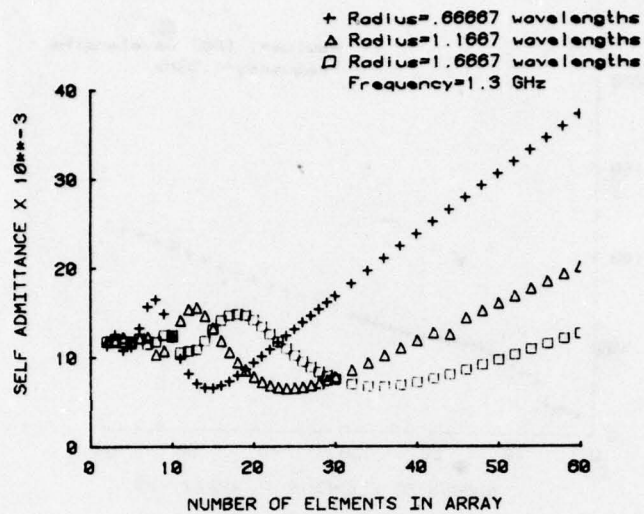
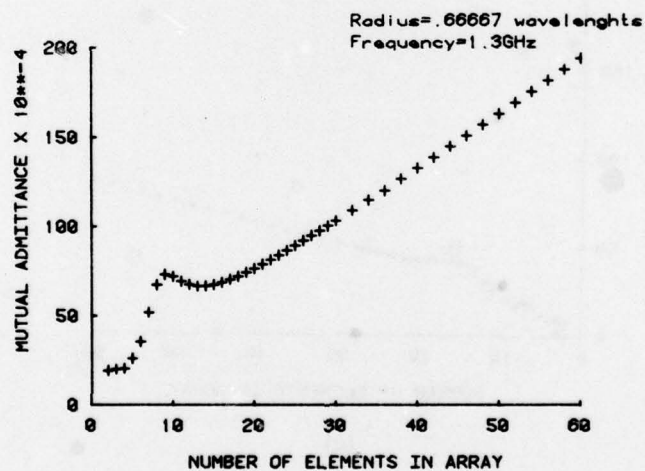
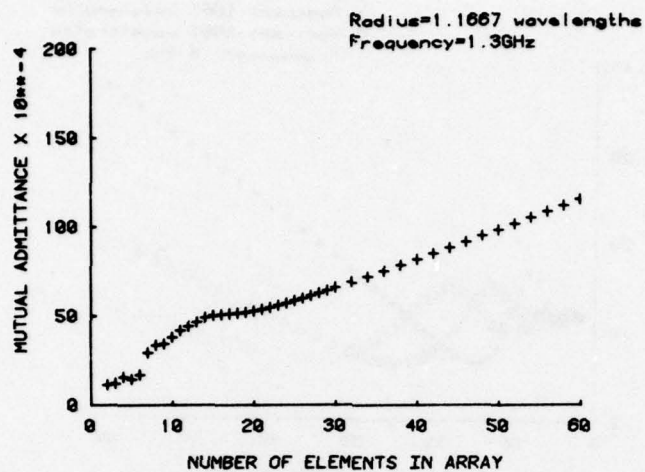


Figure 9. Composite of Figures 8a, 8b, and 8c

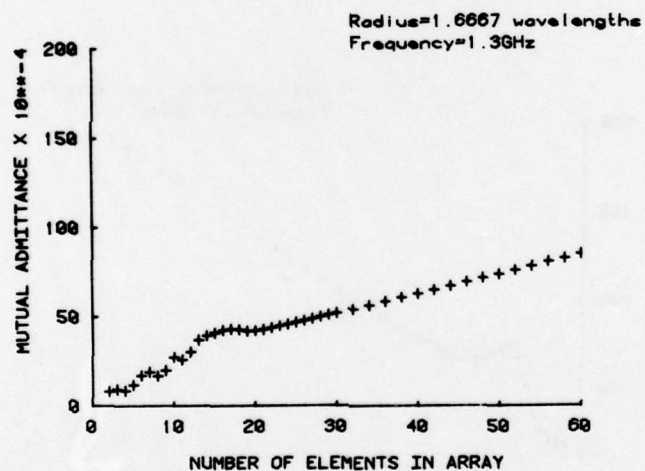


(a)

Figure 10. Magnitude of Mutual Admittance for Varying Number of Elements While Holding Radius and Frequency Constant



(b)



(c)

Figure 10. Magnitude of Mutual Admittance for Varying Number of Elements While Holding Radius and Frequency Constant (Cont)

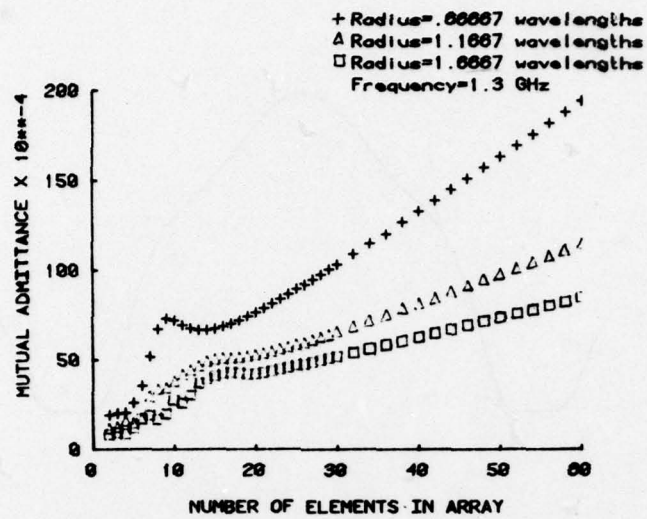


Figure 11. Composite of Figures 10a, 10b, and 10c

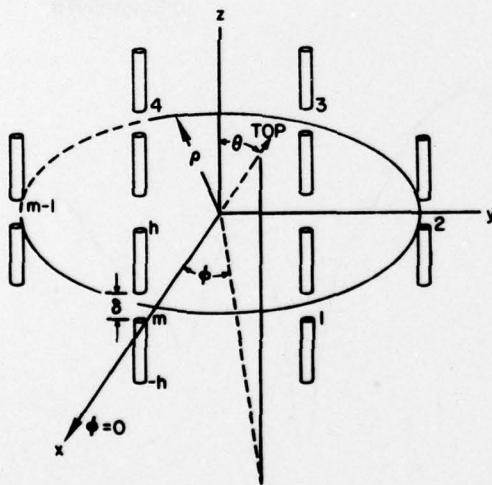


Figure 12. Circular Array Showing Coordinate System Used in Finding Radiation Pattern

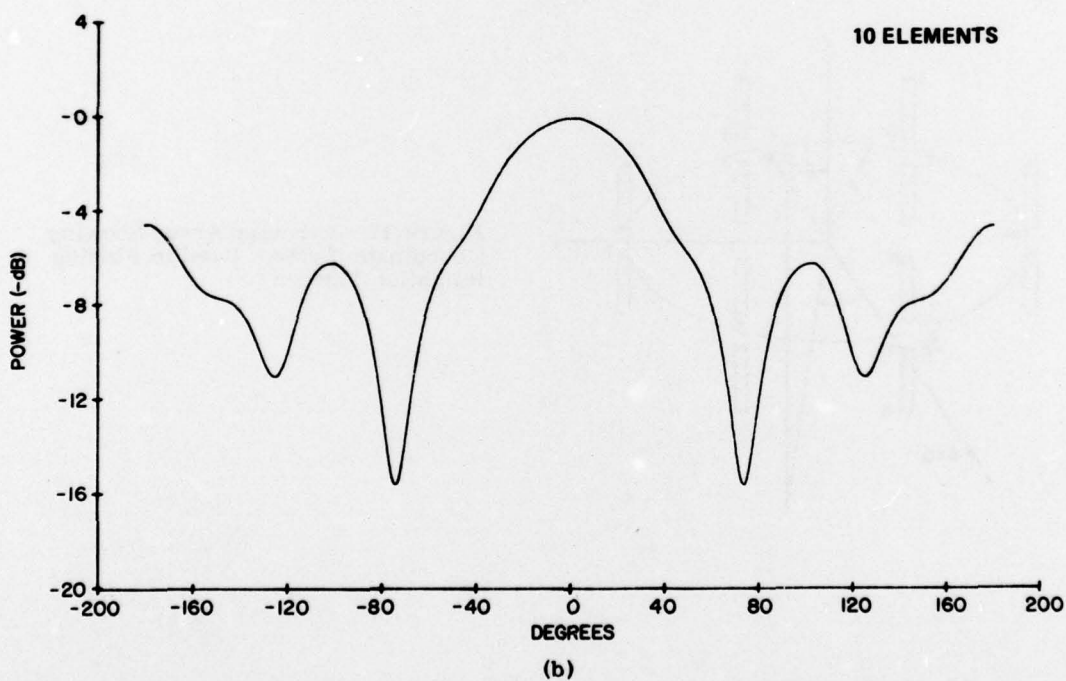
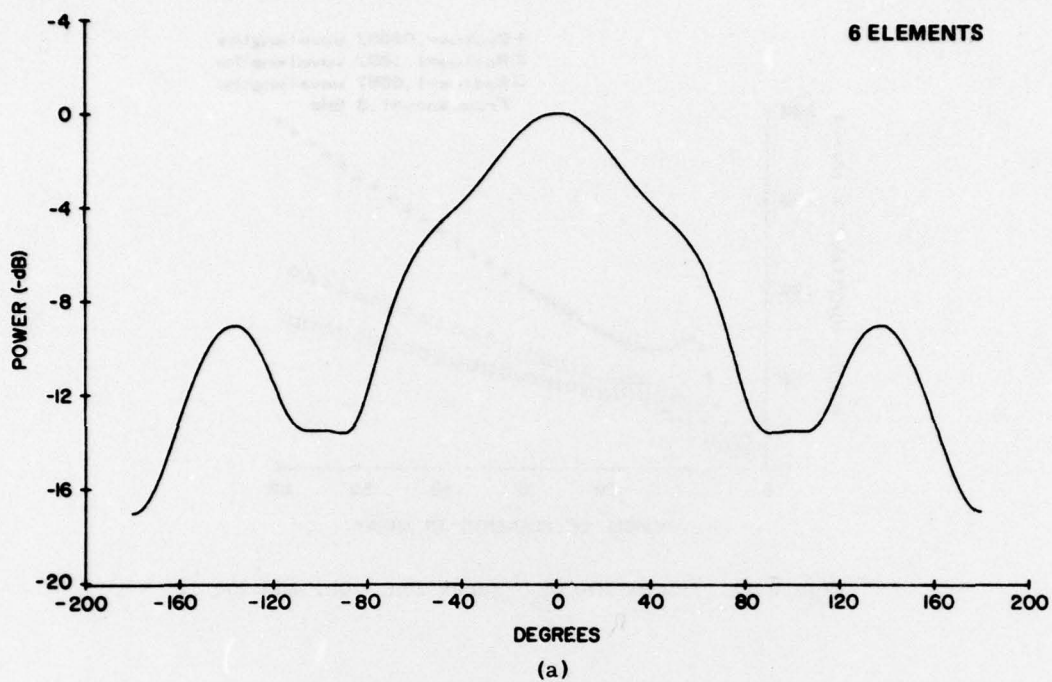


Figure 13. Active Element Patterns for Circular Arrays With 6, 10, 30, 50, and 100 Elements. ($F = 1.3$ GHz, spacing between elements = 0.5λ)

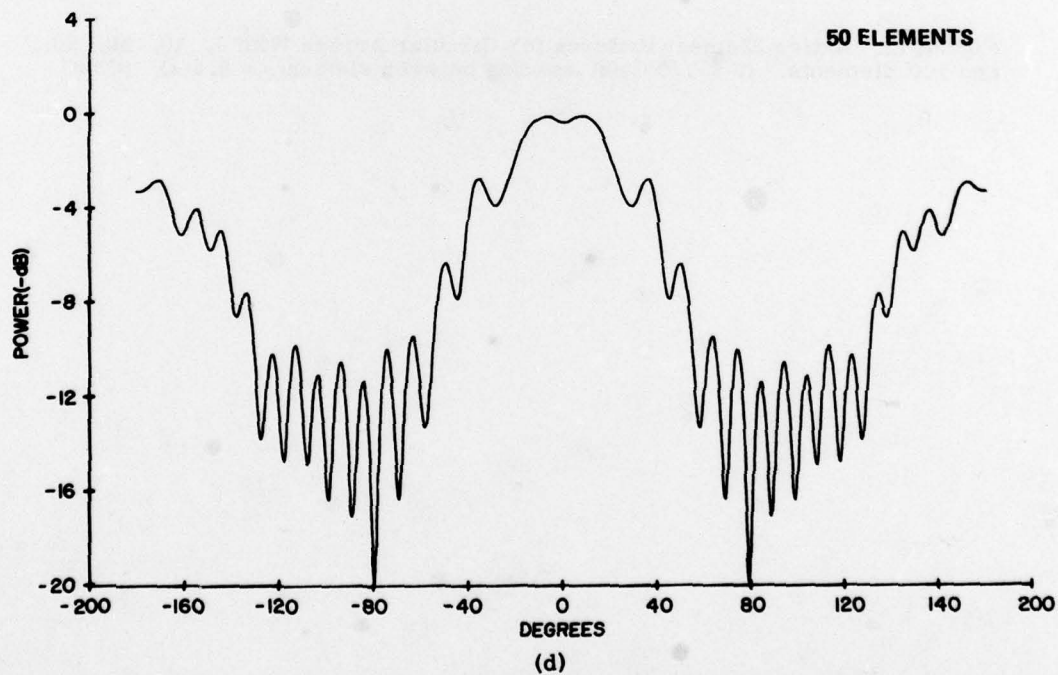
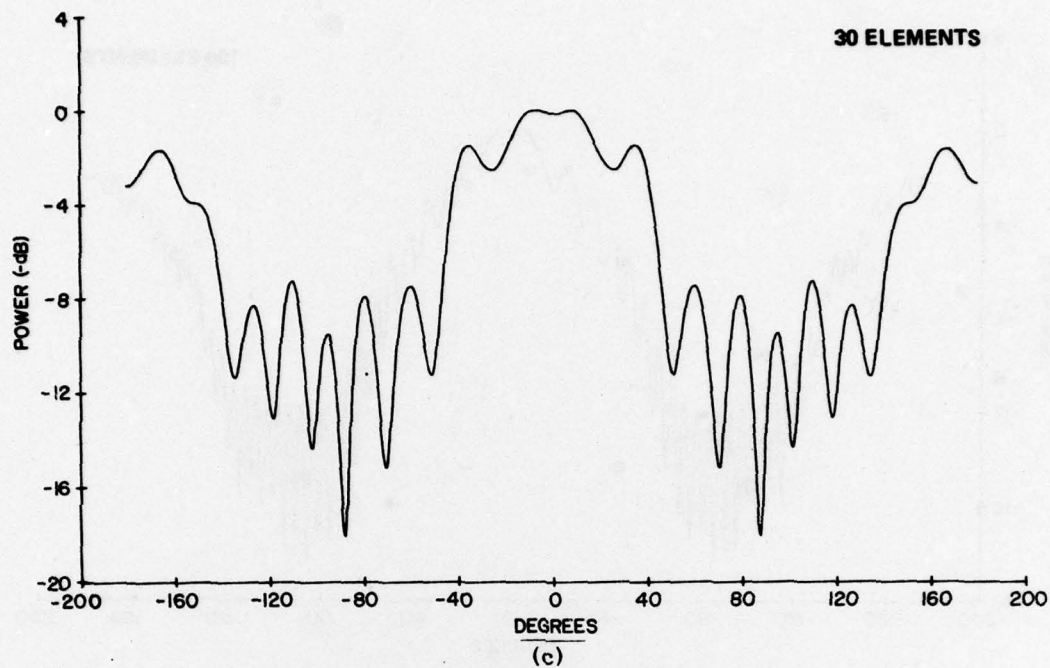


Figure 13. Active Element Patterns for Circular Arrays With 6, 10, 30, 50, and 100 Elements. ($F = 1.3$ GHz, spacing between elements $= 0.5 \lambda$) (Cont)

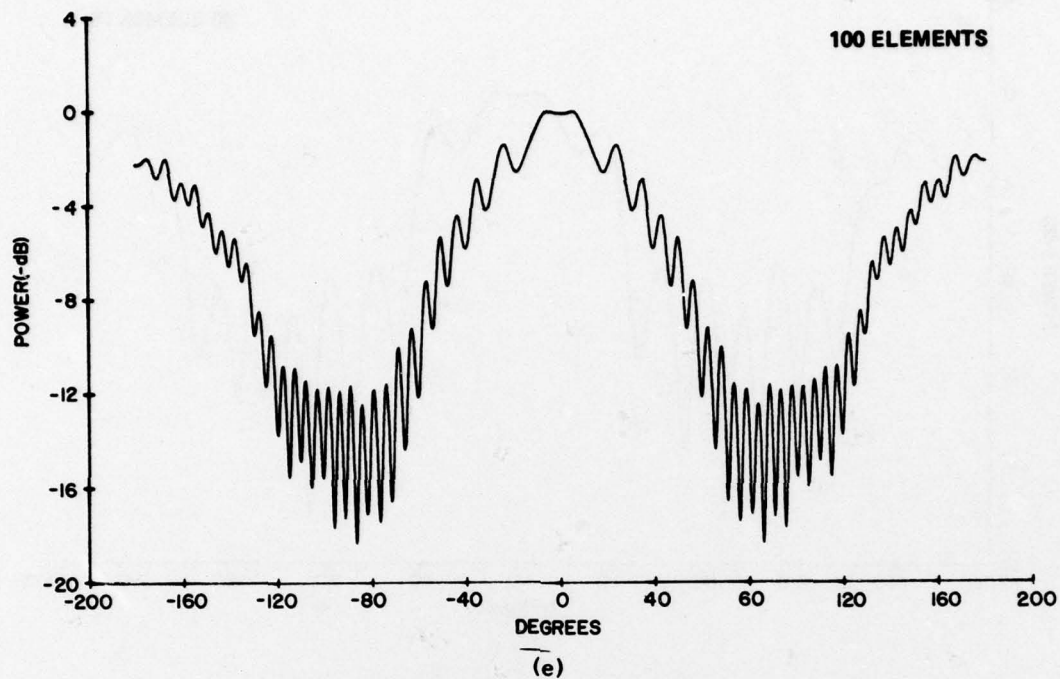


Figure 13. Active Element Patterns for Circular Arrays With 6, 10, 30, 50, and 100 Elements. ($F = 1.3$ GHz, spacing between elements = 0.5λ) (Cont)